ASIAGRAPH 2008 PROCEEDINGS

クジャクの羽のＢＲＤＦレンダリングに関する研究

BRDF Rendering of Peacock Feathers

今村紀之/東京大学 学際情報学府，岩沢俊/東京大学 学際情報学府，河口洋一郎/東京大学 情報学環

Noriyuki Imamura/ the University of Tokyo, Shun Iwasawa/ the University of Tokyo, Yoichiro Kawaguchi/ the University of Tokyo

cask.jp@gmail.com[1], yoichiro@iii.u-tokyo.ac.jp[3]

Abstract: In recent years, a variety of objects have been rendered using computer graphics. This paper focuses on structural color, the simulation of which requires an appreciation of the nature of light. A peacock feather is a good example of a material with structural colors. The bidirectional reflectance distribution function (BRDF) rendering method, which is derived from a model based on both micro and macro structures, was employed in this study. The system closely describes the reflection characteristics both qualitatively and quantitatively and corresponds well with observations.

Keywords: Computer Graphics, Shading, BRDF Rendering, Structural Color

Figure 1: A male Indian peacock.

1. Introduction

The understanding of “color” is widely considered to be one of the most fascinating scientific problems. In addition to issues related to human visual perception, color poses interesting challenges regarding the way it is produced by the surfaces of “colored materials”. In addition to absorption by pigments, colors are also produced by optical phenomena such as interference or the diffraction of light. The latter system of color production is referred to as *structural color* [1], which can be observed at the surface of objects such as, CDs, soap bubbles, the wings of morpho butterflies, and the iridescent plumage of birds such as peacocks: all of these surfaces have the interesting property of variation in the color intensity and reflectance with viewing angle.

In the literature of computer graphics (CG), structural color has usually been represented by simulating the interference of light on a thin film. A CD is represented by simulating the anisotropic characteristics associated with the diffraction of light that arises because of structure of the CD surface [2]. Similarly, the color of a pearl is visualized by modeling the scattering of light and the intereference on multilayered thin films [3]. Similarly, morpho wings are rendered by modeling scales on the wing surface [4]. Although these studies have developed well organized and precise methods for approximating the “micro-level” characteristics associated with the interference of light by thin films, optical phenomena such as “macrostructure” - forms composed of many “micro-structures,” - have long been neglected.

In this paper, using the microstructure of peacock feathers as an example, we propose a method for rendering structural colors that consideres various hues based on physics. Importantly, the model considers both micro- and macrostructural properties of the iridescent feathers, and users can represent various surface attributes in an arbitrary manner by changing the parameters that characterize these structures.

2. Structural Color of Peacock Feathers

The two species of peacock, the Indian peacock (*Pavo cristatus*) (Figure 1) and the green peacock (*Pavo muticus*) belong to the pheasant family, *Phasianidae*. Peacocks have several kinds of differently colored feathers. In this study, we restrict our discussion to two kinds of Indian peacock feathers: the yellow feathers from the ventral area of the upper tail covert and the blue feathers found on most parts of the body.

2.1. Microstructures on a Feather

As shown in Figure 2, a feather is composed of “barbs”, which are branches joined to the main shaft and which are arranged radially. Figure 3 shows the surface of the barbs viewed using both scanning and transmission electron microscopes (SEM/TEM). The barbs themselves are also branched and form “barbules,” which are arranged like a fishbone (Figure 3A).

Barbules are curved along their length and slightly

Figure 2: Glowing yellow and blue feathers (left) [4] and micrographs for each (center and right) [6].

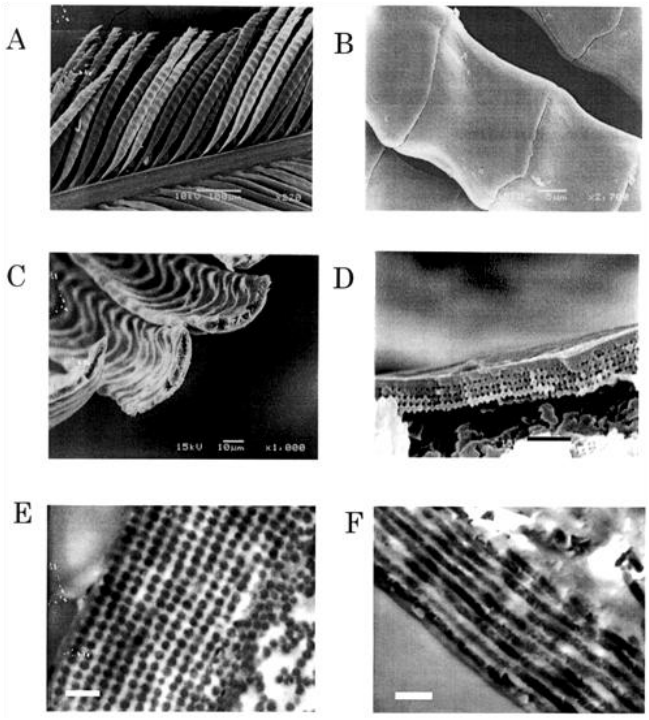

Figure 3: Scanning and transmission electron microscope images of iridescent peacock feathers [5]: A) a barb with many barbules of a blue feather, B) several blocks of a barbule of a blue feather, C) a cross section along the short axis of barbules of a blue feather, D) the cross section along the short axis of a yellow feather under higher magnification, E) TEM image of the cross section along the short axis, F) a longitudinal cross section along of a barbule from a blue feather. The scale bar is 1 μm for D) and 400 nm for E) and F).

twisted at the root. Further, individual barbules are composed of connected blocks, typically measuring 20-30 μm length with the surface of each block being smoothly curved like a saddle (Figure 3B).

In cross section, the short axis of a barbule is crescent-shaped as shown in Figure 3C, and under high magnification, layers of cylindrical structures stacked immediately beneath the surface of barbules can be observed (Figure 3D, E, F). These small cylinders consist of melanin and measure approximately several-μm length and 130-140 nm in radius. The barbules of blue feathers have 8-12 layers with 150 nm interlayer spacing and those of yellow feathers have 3-6 layers with 190 nm spacing between layers [5].

2.2. Reflection Characteristics

Mason [7] was the first to ascribe the structural colors of peacock feathers as being due to multilayer interference by laminated melanin rods in the barbules. As shown in Figure 4, let r be the radius of melanin rod and d be the layer interval. Then the average optical distance per layer D is expressed as:

$$D = d\left\{n_{\mathrm{ml}}\frac{r^2\pi}{2rd} + n_0\left(1 - \frac{r^2\pi}{2rd}\right)\right\} \qquad (1)$$

where n_{ml} is the reflective index of melanin and n_0 is that of air. Assuming that the refractive index of melanin is 2.0

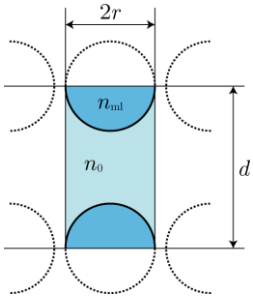

Figure 4: A cross-section view of a barbule along the short axis of a peacock feather

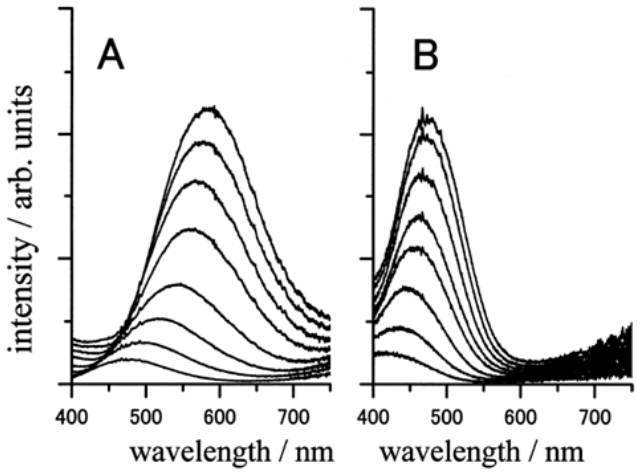

Figure 5: Angular dependence of the reflection spectrum from several barbs containing a numerous barbules for (A) a yellow feather and (B) a blue feather. The incident angle, which is defined as 0°, is roughly normal to the vane. The observation angles are, from top to bottom, 15°, 25°, 35°, 45°, 55°, 65°, 75° and 85° for (A) and (B) [5].

and that of air is 1.0, the average optical distance in a yellow feather is approximately 300.0 nm and that of a blue feather is approximately 252.1 nm from Eq. (1). In this calculation, the parameters are based on the barbule characteristics shown in the preceding subsection.

The optical distances estimated above meet the basic requirements for the constructive interference calculated using the peak wavelength of the reflection spectrum observed by Yoshioka (Figure 5) [5].

Yoshioka also reported the reflection spectrum of one barbule and the reflection pattern obtained from a laser-illuminated barbule for different radiation areas. Based on his research, it was found that barbules have an intensive reflection pattern in a narrow area toward the specular direction. The experiment also characterized the different specular reflection patterns obtained from this multilayer interference over a broad area; up to 80°-120° reflected light angle.

The sharp pattern for the former is considered to be derived from the multilayer interference due to the microstructure of the barbules. On the other hand, the effect on the macrostructure on the latter pattern also needs to be described.

The horizontal diffusion of reflective light is attributed the crescent shape of the cross section of a barbule as shown in Figure 3C. The angle of a crescent arc is usually a maximum of 60°, which corresponds with a horizontal reflection range 120°.

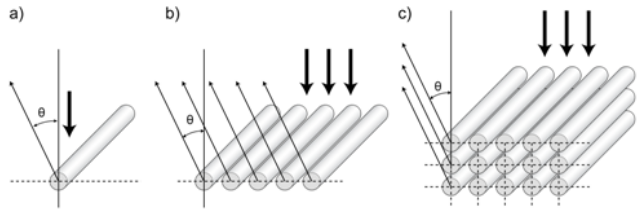

Figure 6: The modeling procedure for barbules along the short axis: a) one rod, b) a one-dimensional array of rods, and c) a two-dimensional array of rods.

Conversely, vertical diffusion is proposed to be caused by two factors: the saddle-like distortion of the blocks that form barbules and diffraction at the discontinuity between melanin rods (both are shown in Figure 3B).

3. Modeling of the Structural Colors

As noted in the preceding section 2.2, describing the variation in the reflected light intensity associated with the structural colors of a peacock feather is difficult using a simple multilayer interference model. This suggests that the following factors need to be considered: 1) Mie scattering on the surface of the melanin rods in the burbules, 2) multilayer interference in the arrays of the melanin rods, 3) anisotropic structure of the barbules along the long and short axis, 4) diffusion in the specular direction caused by the rectangular-shape of the barbules, 5) curvature and torsion of the barbules themselves, 6) distribution of barbules on the barbs, and so on.

In this paper, these factors are classified into three groups depending on the spatial sclae of the phenomena: A) microstructures, B) macrostructures, and C) visible structures.

3.1. Scale A: Microstructures

For microstructures, we consider attributes smaller than the wavelength of visible light, such as Mie scattering and multilayer interference on the melanin rods beneath the barbules.

First, we model the perpendicular oriented bidirectional reflectance distribution function (BRDF) on the micro-structures.

Assuming an infinitely long, light-irradiated rod such as that shown in Figure 6a, the intensity of the diffusion wave u_s at a long distance away are asymptotically derived from the Maxwell equations and expressed as:

$$u_s(r,\theta) \sim \sqrt{\frac{2}{\pi k r}}\left(b_0 + 2\sum_{n=1}^{\infty} b_n \cos n\theta\right) \qquad (2)$$

where r is the distance from the rod, θ is the angle between the incident light and the reflected light, k is the wavenumber, and b_n is a coefficient describing k, the radius of the rod and the refractive index of the rod [8]. Here, k is expressed as $k = 2\pi/\lambda$ in terms of the wavelength of the incident light λ. Note that Eq. (2) is simplified by omitting the factor of the phase shift.

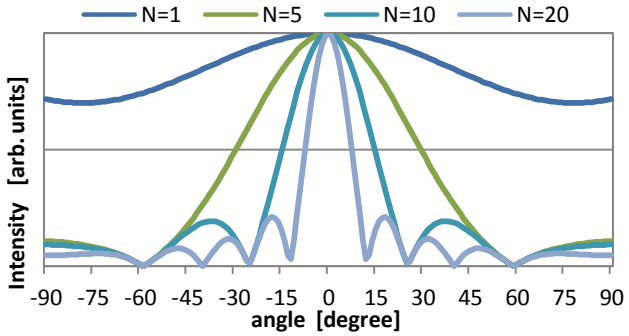

Figure 7: The angular dependence of the reflection intensity calculated for a single and one-dimensional array of infinitely long rods under normal incidence. N is the number of the rods. Intensities are normalized at 0°. The following parameters are used in the calculation: the rod radius of 70nm, the rod interval of 140 nm, wavelength of 600nm and the refractive index of 2.0.

The reflection intensity for a one-dimensional array of infinitely long rods suhch as that shown in Figure 6b can be calculated as the superposition of waves with phase lags. The intensity $I_{N,\theta}$ in terms of the number of rods N and the reflection angle θ can be expressed as:

$$I_{N,\theta} = \frac{1}{N} I_{1,\theta} \left| \sum_{n=1}^{N} e^{i\phi} \right| \qquad (3)$$

$$\phi = \frac{2\pi(n-1)L(\sin\theta_{\text{in}} + \sin\theta_{\text{out}})}{\lambda}$$

where ϕ is the phase lag, L is the rod interval, and $\theta_{\text{in}}, \theta_{\text{out}}$ are the angles of the incidence and reflection. Note that instances of multiple reflections are not considered here.

Figure 7 shows the simulation result for the angular dependence of the reflection intensity determined using Eq. (3). The peak bandwidth for reflection at 0° is observed to get narrower as the number of the rods increases and the diffuse intensity around the larger angle decreases. These effects are considered to be responsible for the sharp pattern shown in the reflection spectrum, which indicates that the rod-array has high flatness and nearly-specular reflection properties due to the regularity of a structure consisting of over ten melanin rods.

Finally, we evaluated light intensiy in a situation in which light falls on a two-dimensional rod array (Figure 6c). Based on the discussion above in Section 3.1, if each one-dimensional array can be regarded as a thin layer, then the structure of a two-dimensional array can be regarded as a thin multilayer. The reflective intensity of the multilayer interference $I(N_d, \theta)$ can be given as:

$$I_{N_d,\theta} = \frac{1}{N_d} I_{1,\theta} \left| \sum_{n=1}^{N_d} e^{i\phi} \right| \qquad (4)$$

$$\phi = \frac{2\pi(n-1)L_d(\cos\theta_{\text{in}} + \cos\theta_{\text{out}})}{\lambda}$$

where N_d is the number of one-dimensional arrays toward the depth direction, L_d is the array interval toward the

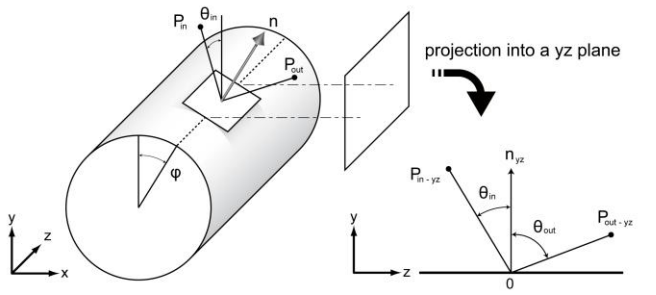

Figure 8: A melanin rod and a longitudinal view of incident and reflection radiation.

depth direction expressed as optical distance, $I_{1,\theta}$ is the intensity in a layer, and ϕ is the phase lag.

The BRDF of the microstructures in the horizontal direction along the long axis of the burbules was formulated as follows:

Using the coordinate axes shown in Figure 8, the reflected light falling on an unit area diffuses depending on ϕ, which is the gradient of the normal direction e.g. "incident light of approximate 0°" of light at the incident point on a rod surface. The intensity of the reflected light I_ϕ is dependent on the probability that light enters the point at gradient ϕ as shown in Eq. (5) below.

$$I_\phi = \cos\phi \sqrt{\frac{1 - \tan\theta_{\text{in}} / \tan\theta_{\text{out}}}{2}} \qquad (5)$$

The light incident into a rod passes through a multilayer formed by the stacked rod layers. In this paper, we use the multilayer model as an approximate approach, with the thickness of the multilayer is averaged by that of rods as shown in Figure 4. Although the diffusion denoted above should be adapted to each stacked layer, for simplicity, diffusion in this study was only calculated once; after the light passes by the multilayer.

3.2. Scale B: Macrostructures

At this scale, we only consider structures that are too large to take on structural colors, but smaller than can be represented using CG. For peacock feathers, diffusion of the reflected light within a barbule is classified as belonging to this scale. Now, let us dissect barbules in the direction of long axis and short axis as in the microstructure phase.

As shown in Figure 9, the cross section of a barbule forms a crescent shape, which affects the direction of reflected light due to the dispersion of the surface normals on the multilayer. In this study, the reflections of the normals from the surface of the crescent have a Gaussian distribution. The distribution, at an arbitrary point, where the gradient of the normal on the multilayer is θ, can be expressed as:

$$k(\theta_{\text{in}})\cos(\theta_{\text{in}} - \theta)\frac{1}{\sqrt{2\pi}\theta}\exp\left(-\frac{\theta^2}{2\theta_0^2}\right) \qquad (6)$$

where θ_{in} is the incident angle, θ_0^2 is the variance, and $k(\theta_{\text{in}})$ is the normalization coefficient. Given that the observations show the range of the gradient to be

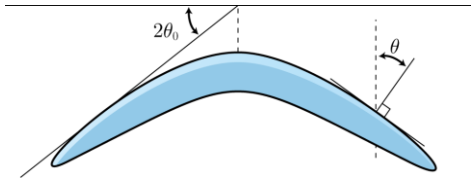

Figure 9: A barbule is a form of crescent shape.

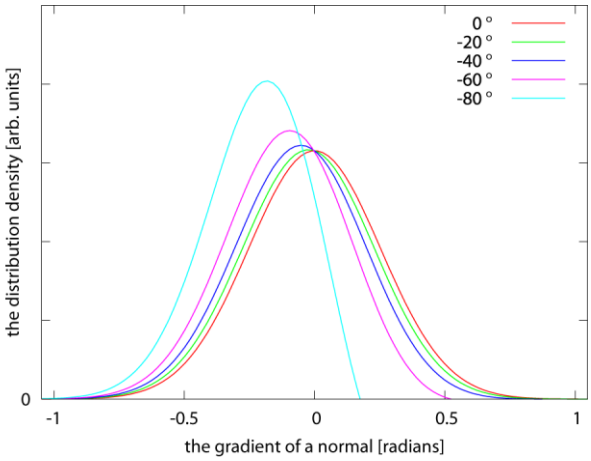

Figure 10: The distribution density of the gradient of normals on the surface of the crescent shape for the different incident angles.

approximately -30°-30°, the θ_0 is estimated to be 15° (Figure 9). The significant level is 4.76% in this estimation. Figure 10 shows the distribution density for the various incident angles using Eq. (6).

In addition, reflected light diffuses on the cross section along the long axis of a barbule because of the curvature of the blocks in the multilayer. As with the cross section of the short axis, the distribution of surface normals along the long axis has an approximately Gaussian distribution. Diffraction caused by the discontinuity between the melanin rods on the barbule surface is also calculated at this scale.

3.3. Scale C: Visible Structures

At this scale, all structural changes that can be described in CG-rendered images can be modeled. Such features include the eyespot of a peacock feather, the direction of barbules, and the deformation of barbs or a feather itself. The parameters for these kinds of phenomena are implemented using reference maps - similar to references image - at the time of rendering. This approach enables users to modify the hue arbitrarily by altering the images.

3.3.1. Alpha Mapping

An alpha map is used to design the shape of a feather. As shown in Figure 11a, the form is represented with grayscale and uses brightness for opacity.

3.3.2. Ocellar Mapping

An ocellar map is a map for defining the shape of the eyespot. The colors of a feather differ depending on factors such as the place where the melanin rods are measured, rod intervals, and the number of rods in an array. In this

implementation, the area of a feather is classified into 6 patterns and the parameters are decided for each group. These patterns are distinguished using the brightness of the map (Figure 11b).

3.3.3. Gradation Mapping

A subtle difference in color appears in the eyespot of a feather, varying from the base of the feather to the apex althogh both belong to the same area in the ocellar map. Such detailed reflection features can be depicted using a gradation map as shown in Figure 11c.

Each pattern in the ocellar map has two reflection properties and the appearance of plumages can be approximated using a linear interpolation of these two properties according to a gradation expression of the map.

3.3.4. Angle Mapping of Barbules

As stated in subsection 2.1, until the edges of the eyespot, the barbs of the feather are joined to the shaft at a slight angle in the same direction as shaft itself. However, at the center of the eyespot, which is at the apex of the shaft, feather barbs are arranged radially. Each barb has many barbules arranged at an angle of 30°-40° like fish bones.

This aeolotropy due to the direction of the barbules on barbs can be represented using an angle map, with the angle of a barbule expressed as brightness (Figure 11d).

3.3.5. Displacement Mapping

The streaky and bumpy surface of the arrays of barbs found on peacock feathers can accurately be realized using displacement mapping, which is popular method in 3DCG (Figure 11e).

3.3.6. Melanin Mapping

The structural colors around the outer edge fade and the take on a brown tinge, which is the actual color of melanin. This is because the microstructures are immature or decrepit near the outer area. In this paper, the intensity of structural color is designed using the same image as that Figure 11f, with brightness used to calculate the ratio of structural colors and melanin brown.

4. Implementation of the BRDF Rendering System

In modeling the micro- and macrostructures, the cross section along the long axis and the short axis are treated separately. These models are integrated using the following equation:

$$I = \frac{\cos 2\psi + 1}{2} f_1(\theta, \phi) - \frac{\cos 2\psi + 1}{2} f_2(\theta, \phi) \qquad (7)$$

where I is the unified reflection intensities, and $f_1(\theta, \phi)$ and $f_2(\theta, \phi)$ are the reflection intensities for the cross section of the long and short axes, respectively.

Figure 12 shows an overview of the BRDF rendering system. Separating the process of inputting parameters and images for the BRDF program itself means that the artists and engineers involved can perform their tasks separately from each other increasing effectiveness.

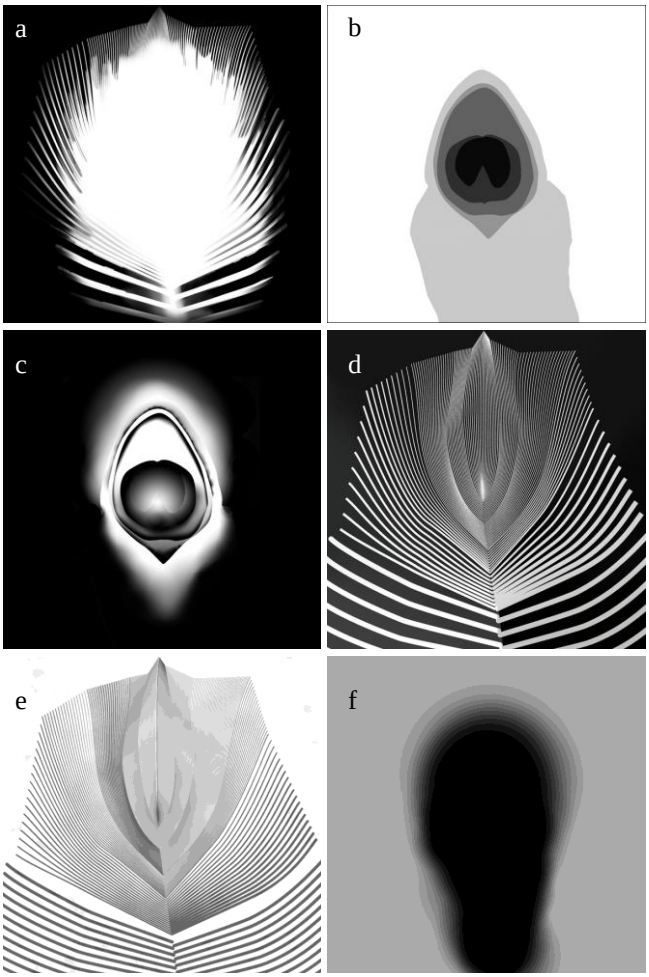

Figure 11: Images for modeling visual structures: a) alpha map, b) ocellar map, c) gradation map, d) angle map of barbules, e) displacement map, and f) melanin map

5. Results and Discussion

Figure 13 shows a comparison between the CG-rendered results generated using the parameters shown in Table 1 and the real feather. The feather was illuminated with sunlight from the right.

The blue and yellow sheen were successfully reproduced in these images. Furthermore, quantitative observations of the spectral reflection intensity obtained using this simulation corresponded with peak peak wavelength, peak width, the feature that the peak wavelength toward the long side for the inclined reflection angles.

Table 1: Parameters for Figure 13. black/white for the grad. map.

ID for	Along long axis			Along short axis		
o. map	L_d	a	N_d	L_d	a	N_d
0 (white)	.19	.075/.070	4	.15	.065	16/18
1	.19	.075	4	.15	.065	16
2	.19 /.17	.075	4/8	.15	.065/.060	16/8
3	.23 /.17	.075	2/16	.15/.17	.070/.060	16
4	.15	.075	4/2	.11	.065	16/4
5 (black)	.11	.060/.075	16	.11	.060/.075	16

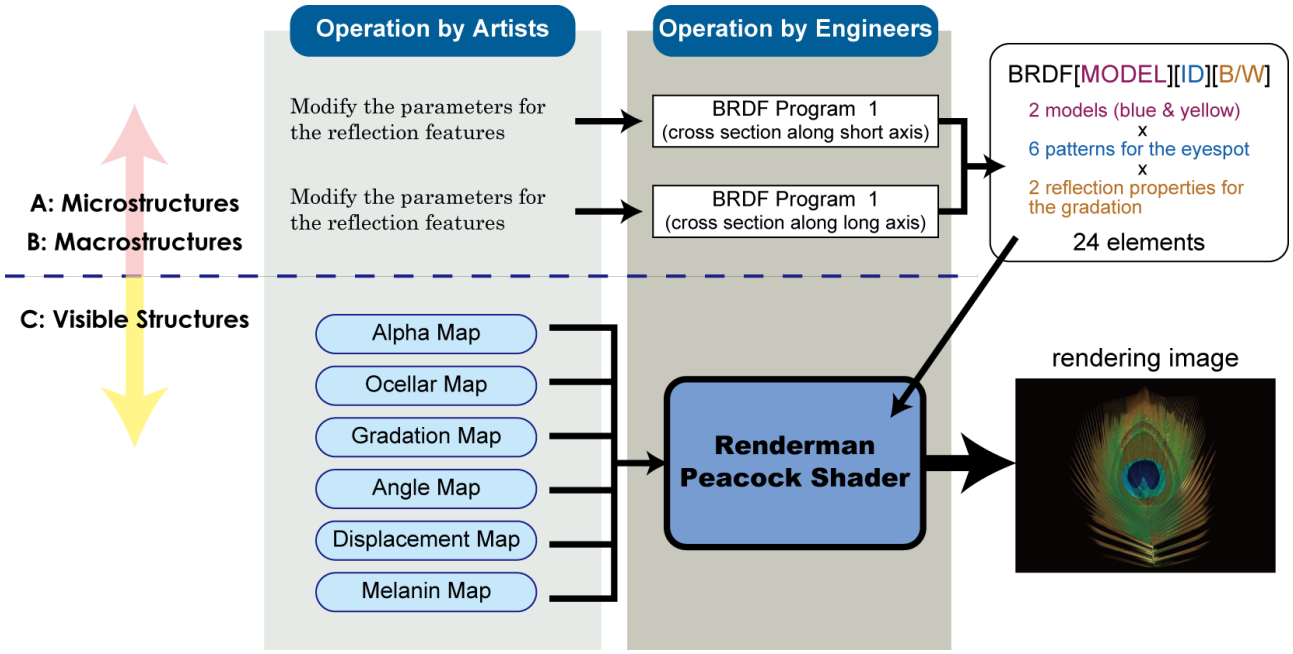

Figure 12: Renderman Peacock Shader system

6. Conclusions

This paper proposed the application of the BRDF method to the rendering of structural colors using peacock feathers as an example. The method considers and integrates both macro- and microstructural feature information of iridescent plumage.

Acknowledgements

We would like to thank CREST of JST for supporting our research.

References

[1] 木下修一, 2001.特集 構造色 総論.In *OplusE* 23, pp298-301
[2] Stam, J., 1999. Diffraction shaders. In *SIGGRAPH '99: Proc. of the 26th annual conf. on CG and interactive techniques*. ACM Press.
[3] Nagata, N., et al., 1997.Modeling and visualization for a pearl-quality evaluation simulator. In *IEEE Transactions on Visualization and Computer Graphics*. IEEE Computer Society.
[4] Iwasawa, S., Shichijo, N., Kawaguchi, Y., 2004. Rendering methods for models with complicated micro structures. In *ICAT 2004 Proc.* VRSJ.
[5] Yoshioka, S., et al., 2004. Structural color of peacock feathers. In Structural Colors in Biological Systems, Osaka Univ. Press.
[6] Society of Structural Color, http://mph.fbs.osaka-u.ac.jp/~ssc/e-birds.html.
[7] Mason, C. W., 1923. Structural colors in feathers, In T*he J. of Phys. Chem.* American Chemical Society.
[8] van de Hulst, H. C., 1957. *Light scattering by Small Particles*, Jhon Wiley & Sons. New York.

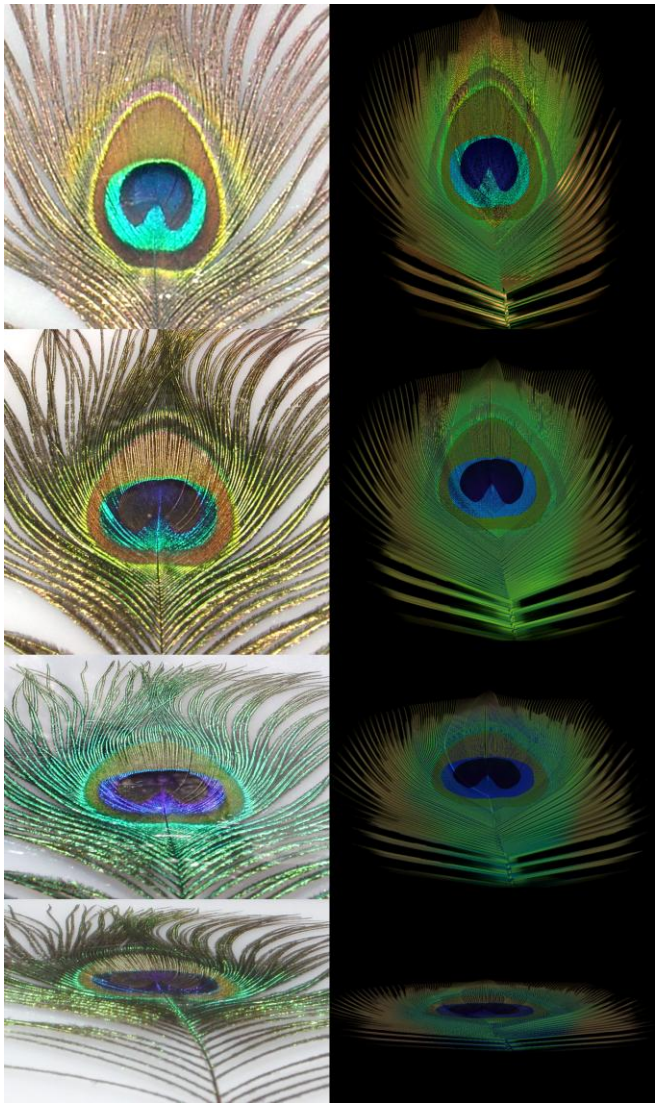

Figure 13: A real object of a peacock feather (left) and the rendering results (right)